The Astrophysical Journal, 581:770–775, 2002 December 10

MEASUREMENTS OF [C I] EMISSION FROM COMET HALE-BOPP

R. J. Oliversen,[1,2] N. Doane,[2,3,4] F. Scherb,[2,5] W. M. Harris,[6] and J. P. Morgenthaler[5]

Received 2001 July 19; accepted 2002 August 12

ABSTRACT

We present quantitative measurements of cometary [C I] 9850 Å emission obtained during observations of comet Hale-Bopp (C/1995 O1) in 1997 March and April. The observations were carried out using a high-resolution ($\lambda/\Delta\lambda \approx 40,000$) Fabry-Pérot/CCD spectrometer at the McMath-Pierce Solar telescope on Kitt Peak. This forbidden line, the carbon analog of [O I] 6300 Å, is emitted in the radiative decay of $C(^1D)$ atoms. In the absence of other sources and sinks, [C I] 9850 Å emission can be used as a direct tracer of CO photodissociation in comets. However, in Hale-Bopp's large, dense coma, other processes, such as collisional excitation of ground-state $C(^3P)$, dissociative recombination of CO^+, and collisional dissociation of CO and CO_2 may produce significant amounts of $C(^1D)$. The long $C(^1D)$ radiative lifetime (~4000 s) makes collisional deexcitation (quenching) the primary loss mechanism in the inner coma. Thus, a detailed, self-consistent global model of collisional and photochemical interactions is necessary to fully account for [C I] 9850 Å emission in comet Hale-Bopp.

Subject heading: comets: individual (Hale-Bopp (C/1995 O1))

1. INTRODUCTION

After water, carbon monoxide is believed to be the next most abundant molecular species in most comets. In interstellar molecular clouds, its abundance is exceeded only by molecular hydrogen, and it is used as a tracer of H_2 in such clouds. Because comets are presumably composed of interstellar cloud material that was processed in the early solar nebula, studies of the density, state, and photochemistry of CO in cometary comae offer an opportunity to constrain formation and evolution histories of cometary nuclei.

Much recent work in the study of cometary CO has focused on its state in the comet nucleus and its subsequent interactions in the coma. Studies of ultraviolet emission from the CO fourth positive (Festou 1984) and Cameron bands (Weaver, Feldman, & McPhate 1994; Feldman et al. 1997) have shown that the abundance of CO and the state in which it is bound in comet nuclei vary from comet to comet. In particular, the derived CO/CO_2 ratio is found to vary by more than a factor of 2 (Feldman et al. 1997), a difference that may be indicative of formation conditions at different locations in the solar nebula, the evolution of surface ices on nuclei that have undergone multiple solar encounters, or a combination of these and other effects. Other studies of CO and its daughter products suggest a complex evolution within the coma that is not explained by simple radial expansion and photochemistry (Tozzi, Feldman, & Festou 1998). Thus, photodissociation daughters are a diagnostic of both the parent identity (e.g., CO_2 vs. CO) and conditions in the coma.

One tracer of the CO production rate Q(CO) and the CO distribution in the coma is emission from $C(^1D)$ via the forbidden [C I] lines at 9823 and 9850 Å (Fig. 1). These lines are analogous to the well-studied [O I] lines at 6300 and 6364 Å and offer a comparable opportunity to study the production rates and photochemical evolution of the parent molecules (e.g., Schultz et al. 1992). The $C(^1D)$ in the coma is produced from photodissociation of CO (Huebner, Keady, & Lyon 1992), electron impact on ground-state $[C(^3P)]$ carbon, and dissociative recombination of CO^+ (Feldman 1978; Bhardwaj 1999). Where photodissociation dominates over other processes, [C I] emission is a tracer of the local CO column density. With a large cross section for low-energy collisional excitation, $C(^1D)$ is an excellent probe of regions of high gas and electron density in the coma. For very active comets, such as Hale-Bopp, collisions with electrons, ions, and neutrals in the high-density coma will significantly quench $C(^1D)$, which has a relatively long radiative lifetime (4077 s; Hibbert et al. 1993). In principle, measurements of the two-dimensional distributions of [C I] 9823, 9850 Å emissions would distinguish among these various sources and sinks, as well as constrain the abundance, distribution, and evolution of CO. Detection of [C I] 9850 Å emission in comet Halley was reported by G. Münch et al. to the International Halley Watch hotline (Tozzi et al. 1998). Münch et al. assigned a preliminary surface brightness of 8 ± 1 rayleighs [$1\ \mathrm{R} = 10^6/(4\pi)$ photons $s^{-1}\ cm^{-2}\ sr^{-1}$] to their observation, but neither the spectrum nor a final calibrated brightness value was subsequently published.

More commonly, measurements of cometary $C(^1D)$ are made using observations of the ^1D–^1P emission line at 1931 Å (Fig. 1), which is produced by resonance fluorescence of solar radiation by $C(^1D)$ atoms in the coma (Feldman 1978; Tozzi et al. 1998). Using archival *International Ultraviolet Explorer* UV spectra of several comets, Tozzi et al. (1998) found a strong correlation between $C(^1D)$ and CO production rates. They inferred that CO photodissociation was the primary source of the observed $C(^1D)$ atoms in those cometary comae. Consequently, at least for the type of comets

[1] NASA Goddard Space Flight Center, Greenbelt, MD 20771; ron@midnight.gsfc.nasa.gov.

[2] Visiting Astronomer at the National Solar Observatory, operated by the Association for Research in Astronomy, under contract to the National Science Foundation.

[3] NASA Goddard Space Flight Center, Greenbelt, MD 20771.

[4] Currently at Department of Astronomy, University of Wisconsin, Madison, WI 53706; doane@astro.wisc.edu.

[5] Department of Physics, University of Wisconsin, Madison, WI 53706; scherb@physics.wisc.edu, jpmorgen@alum.mit.edu.

[6] Space Astronomy Lab, University of Wisconsin, Madison, WI 53706; wharris@sal.wisc.edu.

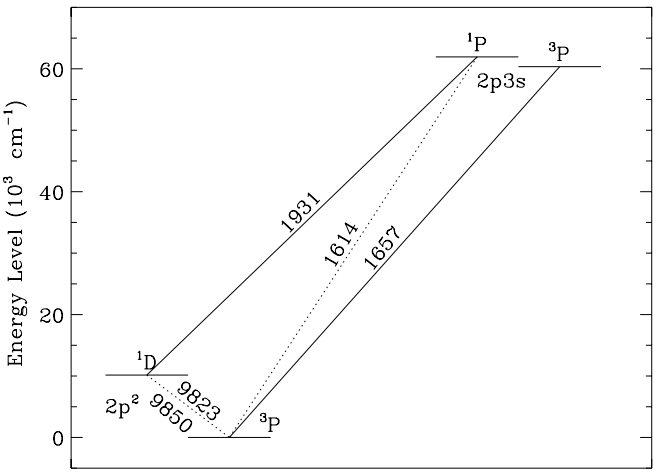

FIG. 1.—Partial Grotrian diagram of atomic carbon. Allowed transitions are indicated by solid lines; forbidden transitions are dotted lines; transition wavelengths are in units of angstroms.

studied by Tozzi et al. (1998), ground-based observations of [C I] 9850 Å emission could be used to derive the cometary CO production rate in the same way [O I] 6300 Å observations are used to determine the water production rate (Fink & Di Santi 1990; Schultz et al. 1992; Smyth et al. 1995; Morgenthaler et al. 2001). We find, however, that because of Hale-Bopp's unusually high gas production rate and the much longer metastable lifetime of C(^1D) compared to O(^1D), collisional processes may be more significant in determining the observed C(^1D), at least within the $\sim 2.7 \times 10^5$ km field of view (FOV) of our instrument. A similar conclusion was reached by Feldman (1978) when analyzing UV sounding rocket observations of C I 1931 Å in comet C/1975 V1-A (West), which, like Hale-Bopp, had a very high density gas coma.

2. OBSERVATIONS

The observations were carried out at the National Solar Observatory (NSO) McMath-Pierce 1.5 m main telescope on Kitt Peak, using a 50 mm dual-etalon Fabry-Pérot (FP) spectrometer (Roesler 1974) with a 4′.1 diameter FOV (Morgenthaler et al. 2001). FP spectrometers are particularly well suited for high spectral resolution observations of extended faint sources (Roesler, Reynolds, & Scherb 1995), and the large FOV usually includes a substantial fraction of the total emission from the C(^1D) or O(^1D) atoms in the coma (Morgenthaler et al. 2001). The first observing run, 1997 March 9–10, produced two nights of [C I] 9850 Å data, and the second run, 1997 April 7–19, yielded 11 nights of data (Table 1). Hale-Bopp [O I] 6300 Å spectra were also recorded on most of these nights and are presented elsewhere (Morgenthaler et al. 2001).

Instrument spectral tuning and wavelength calibrations were done using the argon 9854.09 and 9849.46 Å lines from a Sn/Ar hollow cathode lamp. Flat fields were taken using an internal white light source reflected off a diffusing screen. Intensity calibrations were obtained from observations of [C I] 9850 Å emission from the Orion Nebula (M42), for which a surface brightness map was published by Münch & Hippelein (1982). Although M42 measurements could not be obtained on every night, auxiliary observations of α Boo provided a nearly continuous record of overall relative system response to the continuum around 9850 Å, except on April 10 and 19, when clouds rolled in after the comet observations, preventing calibration measurements for those evenings. The FP/CCD was used in the "annular summing" mode, in which the FP spectral ring pattern (rather than the

TABLE 1
SUMMARY OF OBSERVATIONS

Date	UT Time[a]	Air Mass	FOV[b] (10^5 km)	R[c] (AU)	$\dot{R}$[d] (km s^{-1})	Δ[e] (AU)	$\dot{\Delta}$[f] (km s^{-1})	Intensity[g] (R)
1997 Mar 9.....	12:32–12:38	3.2–2.9	2.56	0.9989	−12.25	1.3822	−17.50	102 ± 10
1997 Mar 10.....	12:53–13:05	2.6–2.4	2.51	0.9919	−11.28	1.3723	−16.20	111 ± 23
1997 Apr 7	2:27	3.4	2.58	0.9204	3.614	1.4079	19.55	132 ± 13
1997 Apr 8	3:15	2.3	2.60	0.9226	4.206	1.4193	20.46	196 ± 32
1997 Apr 9	2:55–3:10	2.1–2.9	2.62	0.9253	4.785	1.4311	21.32	164 ± 31
1997 Apr 10.....	2:44–3:09	2.0–3.5	2.65	0.9282	5.366	1.4436	22.15	180 ± 79[h]
1997 Apr 11.....	2:34–2:57	3.4–4.4	2.67	0.9314	5.926	1.4562	22.90	120 ± 16
1997 Apr 12.....	2:28–3:07	2.0–2.7	2.69	0.9350	6.487	1.4694	23.63	130 ± 26[i]
1997 Apr 13.....	2:50–3:01	3.9–4.8	2.72	0.9389	7.046	1.4833	24.32	170 ± 12[i]
1997 Apr 14.....	3:06–3:26	2.7–3.2	2.74	0.9432	7.591	1.4974	24.97	177 ± 66[i]
1997 Apr 15.....	2:52–3:14	2.4–2.9	2.77	0.9477	8.122	1.5118	25.56	183 ± 33[i]
1997 Apr 16.....	3:38	3.6–4.9	2.80	0.9526	8.657	1.5269	26.12	254 ± 14
1997 Apr 19.....	2:31–3:06	1.9–2.7	2.88	0.9688	10.143	1.5725	27.52	220 ± 12[h]

[a] Beginning and ending times; typical exposures were 5–10 minutes.
[b] Field-of-view diameter.
[c] Heliocentric distance.
[d] Heliocentric velocity.
[e] Geocentric distance.
[f] Geocentric velocity.
[g] [C I] 9850 Å intensity. Errors are the standard deviation of the individual measurements for each night, except on nights with only one measurement (indicated with a single time in the "UT Time Range" column), where the statistical error from the spectral fit was used.
[h] Calibration assumes average M42 signal measured in April.
[i] Only α Boo calibration data available.

sky) was imaged onto the CCD detector (Coakley & Roesler 1994). Therefore, no spatial information within the FOV was obtained. Each CCD image had a wavelength coverage of 5.5 Å (170 km s^{-1}), with resolution of 0.25 Å (7.5 km s^{-1}) toward the red end of the spectrum and a slightly lower resolution (by 20%) toward the blue end (§ 3.1).

Guiding on the comet head to a precision of better than 5″ was accomplished by directing light ($\lambda < 5800$ Å) to a guide camera from a dichroic beam splitter placed near the image of the primary mirror. Differential refraction (<2″) between the guide camera and the CCD was negligible for our FOV. On twelve occasions, observations were obtained with the FOV centered approximately 5.′2 sunward or antisunward of the comet nucleus. The off-comet head observations were unguided, and the telescope drifted ~30″–60″ from its initial offset during an exposure. This drift was likely due to atmospheric refraction not modeled in the telescope drive system. However, this drift was small enough to keep the sunward/antisunward FOVs from overlapping the head-centered FOV.

3. DATA REDUCTION

3.1. *Image Processing*

Each FP/CCD image was subjected to standard bias, flat-field, and cosmic-ray processing. The telescope primary (No. 2) mirror, imaged directly onto the CCD detector, was conjugate with the FP ring pattern; thus, each spectral element was mapped onto a particular part of the mirror. Several effects changed the illumination of the primary mirror: declination foreshortening of the heliostat (No. 1) mirror, a chip in the primary mirror, and partial blocking of the FOV by the McMath-Pierce east and west auxiliary telescopes (Fig. 2). These effects were masked out of each image so that the annular sum included the maximum unattenuated comet and sky signals. Atmospheric lines seen outside the mirror image are the result of skylight reflecting off the white superstructure of the McMath-Pierce heliostat mirror.

The center of each ring pattern was found, and the distance from the center of the ring pattern was calculated for rings of 1 km s^{-1} spectral bins (red in the center, blue to the

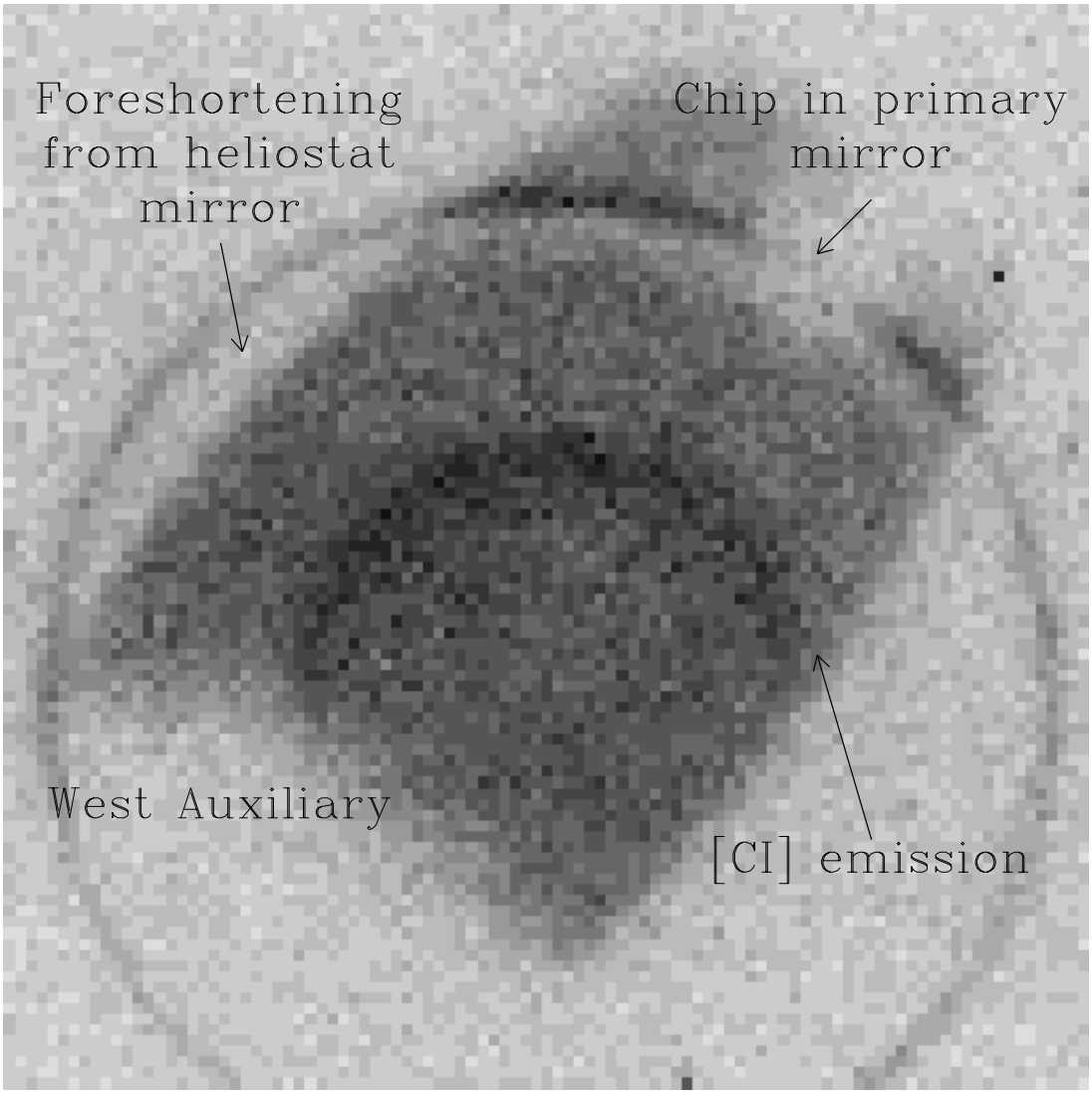

FIG. 2.—Bias-subtracted, flat-fielded image of the FP ring pattern from 1997 April 16 with cosmic rays removed. As described in the text, the telescope primary (No. 2) and heliostat (No. 1) mirrors are imaged on the detector together with various obstructions. The ring that extends beyond the mirror image is terrestrial OH 9848.48 Å, reflecting off the heliostat superstructure.

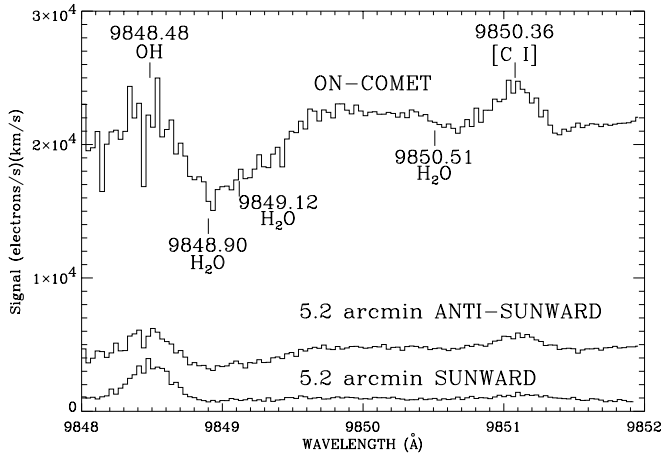

FIG. 3.—Extracted spectra of Comet Hale-Bopp on 1997 April 10

outside). The CCD pixels were binned 2×2 for faster acquisition of the images (due to short observing windows) and easier detection of the [C I] emission. As a result of the binning, the outer FP spectral rings were less than a binned pixel wide, which broadened and introduced a weak wavelength dependence in the effective instrumental spectral profile. Sample extracted spectra are shown in Figure 3.

3.2. *Spectral Fitting*

The spectra were analyzed using a nonlinear least-squares fitting program that utilized multiple spectral lines with Voigt profiles and a continuum up to a quadratic function. The weaker lines, including the cometary [C I] line, were typically fitted only with Gaussian functions. Specific wavelengths for terrestrial atmospheric OH emission (Osterbrock, Fulbright, & Bida 1997) and H_2O absorption lines (Swensson et al. 1970) were linked together in the fitting procedure to reduce the number of free parameters. No solar spectral features in the continuum due to scattering by cometary dust, nor any other cometary lines, were seen or included in the model.

3.3. *Systematic Errors*

Nonuniform illumination of the primary (No. 2) telescope mirror, its variation with telescope hour angle, and, on some spectra, inadequate spectral coverage of the continuum to the red of the [C I] 9850 Å line were the primary sources of systematic error in the measured intensity of the line. Because of nonuniform illumination, not every spectral element (e.g., ring in the Fabry-Pérot pattern) received equal exposure (Fig. 2). This effect was corrected by masking out the affected areas and averaging the remaining signal in each spectral element (§ 3.1). Systematic differences in spectra due to placement errors of the mask were minimized by using the telescope hour angle and declination to calculate the orientation and size of the mask. However, masking the areas vignetted by the auxiliary telescopes was more difficult and less precise, as the auxiliary telescopes were not in focus. The overall shape of a spectrum was affected by the amount and distribution of light scattered into the telescope beam from the heliostat superstructure and by a small variable misalignment between the etalons induced by pressure changes in the individual etalon chambers (Morgenthaler et al. 2002). The scattered light induced low spatial frequency variations across the primary mirror, was sensitive to the telescope orientation and twilight sky background gradients, and was variable as a function of time. Therefore, it was not possible to obtain sky flats that matched comet observing conditions, so internal flats were used, which, although not perfect, gave more consistent results. The residual effect of the scattered light, auxiliary telescope masking, and etalon misalignment problems was to induce artificial variations in the spectral continuum, with the red end of the spectrum being most sensitive. The effect was most severe for those spectra with a small amount of continuum coverage to the red of the [C I] line.

Another source of systematic error came from variation in atmospheric conditions, especially transparency, during cometary, M42, and α Boo observations. This problem is most serious for observations at large air mass, especially those in April, some of which were taken only 30 minutes after sunset, when the atmosphere was cooling rapidly. As noted in Table 1, on some nights α Boo, which was observed at low air mass, was the only calibration target at [C I], so the cometary [C I] intensities on these nights are more likely to have systematic errors.

Because of these effects, we assign a systematic error of 50% to our absolute [C I] 9850 Å intensities. We note, however, that the scatter in [C I] 9850 Å intensity values in Table 1 for adjacent nights is only slightly larger than the statistical uncertainties (quoted errors) derived from each night's observations, so relative systematic errors are likely less than 25%.

4. RESULTS

There is a substantial asymmetry between the tailward and sunward [C I] intensities (see Fig. 3); the average ratio of sunward to head-centered intensities is 0.10 ± 0.04 (six observations) versus 0.36 ± 0.09 (six observations) for the antisunward to head-centered ratio. We used a simple spherically symmetric Haser photodissociation model (Haser 1957) and the FOV sensitivity map derived by Morgenthaler et al. (2001) to predict a radial distribution of the [C I] 9850 Å emission. With Haser model outflow velocities similar to those derived from fits to [O I] 6300 Å and OH data (Harris et al. 2002; Morgenthaler et al. 2001) and a CO photodissociative lifetime estimated to be 10 times that of H_2O (Tozzi et al. 1998), the predicted [C I] 9850 Å distribution is very flat. The model off-head to on-head intensity ratio is close to our observed value in the antisunward direction, but is much larger than the observed sunward value. Assuming a spherical model and the Tozzi et al. (1998) CO photodissociation lifetime, the observed sunward to head-centered ratio could only be reached if the telescope FOV was centered more than 15′ from the head, which is unlikely, given the 5.′2 off-head starting distance and the maximum 1′ per exposure unguided telescope drift (§ 2).

In order to provide a context in which we can compare our results with other observations of Hale-Bopp, it is useful to employ a hypothetical CO photodissociation model to derive a nominal value of Q(CO) from our [C I] 9850 Å measurements. The quantities necessary for this calculation are the total $C(^1D)$ production rate $Q[C(^1D)]$ (see Table 2) and the $CO + h\nu \rightarrow C(^1D) + O(^1D)$ branching ratio (BR). Our off-head observations show that the FOV was not large enough to detect all of the [C I] emission from Hale-Bopp, so we must estimate an aperture correction (AC). The Haser

TABLE 2
PHOTODISSOCIATION LOWER LIMITS TO AVERAGE PRODUCTION RATES OF C(^1D) AND CO IN 1997 MARCH AND APRIL

Date	Q[C(^1D)][a] (10^{28} s^{-1})	Q(CO)[a,b] (10^{28} s^{-1})
Mar 9–10	>14	>46
Apr 7–19	>26	>87

[a] $Q[\mathrm{C}(^1D)] = (4/3)(4\pi\Delta^2\Omega I_{9850})\mathrm{AC}$ (e.g., Schultz et al. 1992), where Δ is the geocentric distance to the comet in cm, Ω is the solid angle of the FOV in steradians, I_{9850} is the average intensity over the FOV in photons s^{-1} cm^{-2} sr^{-1}, and AC > 2.

[b] $Q(\mathrm{CO}) = Q[\mathrm{C}(^1D)]/\mathrm{BR}$ where the $\mathrm{CO} + h\nu \rightarrow \mathrm{C}(^1D) + \mathrm{O}(^1D)$ branching ratio, BR < 0.3 (Tozzi et al. 1998).

model discussed above suggests AC > 10; our sunward data suggest AC > 2. Tozzi et al. (1998) estimate that BR is between 0.10 and 0.30. Using AC = 2 and BR = 0.3, we find the lower limits to Q(CO) shown in Table 2, assuming no additional sources or sinks of CO.

Using long-slit CSHELL spectra, Di Santi et al. (2001) found $Q(\mathrm{CO}) = (2.07 \pm 0.2) \times 10^{30} R^{-1.66\pm0.22}$ s^{-1}, where R is the heliocentric distance in AU. Di Santi et al. (2001) found that about one-half of the CO in Hale-Bopp came from a distributed source with a scale length greater than $(6–7) \times 10^3$ km (small compared to our FOV). On 1997 April 6, the UV measurements of McPhate et al. (1999) yielded $Q(\mathrm{CO}) = (3.3 \pm 0.4) \times 10^{30}$ s^{-1}, and from April 10–30, the radio measurements of Biver et al. (1997) determined Q(CO) to be $(1.6 \pm 0.5) \times 10^{30}$ s^{-1}. Thus, our photodissociation-derived Q(CO) lower limits in Table 2 are not inconsistent with other Q(CO) values.

5. DISCUSSION

A possible source of the sunward-tailward [C I] asymmetry is dissociative recombination of CO^+ (Feldman 1978). Sounding rocket UV spectroscopic observations of comet C/1975 V1-A (West) (Feldman & Brune 1976) showed a strong C I 1931 Å emission feature, which Feldman (1978) attributed to this mechanism. We note, however, that similar, although much less pronounced, tailward extensions exist in the OH (Harris et al. 2002) and O(^1D) (Morgenthaler et al. 2001) data, which would not be related to CO^+. Some effect in the sunward coma could be suppressing the [C I] emission or modifying its spatial distribution. Support for the latter comes from the dusty gas model of Combi et al. (1999), which predicts a focused neutral gas deceleration in the sunward direction due to dust mass loading, which, if sufficiently large, could cause the asymmetry we see. However, the OH images of Harris et al. (2002) and [O I] 6300 Å images of Morgenthaler et al. (2001) do not show this to be a significant effect.

By adopting the CO photodissociation model suggested by Tozzi et al. (1998), we derive a lower limit to Q(CO) (Table 2) that is similar to other results (Di Santi et al. 2001; McPhate et al. 1999; Biver et al. 1997). However, this agreement may be fortuitous, since the spatial distribution of the emission in the sunward direction follows a steeper radial gradient than the Tozzi et al. (1998) results suggest. The source of this discrepancy may be related to the overall high gas production rate from Hale-Bopp. The radial extent of Hale-Bopp's collision sphere ($r \sim 10^5$ km; e.g., Whipple & Huebner 1976; Combi et al. 1999; Harris et al. 2002) and the long C(^1D) radiative lifetime both suggest that [C I] emission is more likely to be governed predominantly by processes such as (1) electron impact dissociation of CO and CO_2, (2) dissociative recombination of CO^+, (3) electron, ion, and neutral collisional deexcitation (quenching) of C(^1D), and (4) electron collisional excitation of C(^3P) to the C(^1D) excited state (Tozzi et al. 1998; Bhardwaj 1999). The importance of these other processes relative to photodissociation depends on the total gas production rate and the degree to which collisions dominate over the region sampled. For example, the model results of Bhardwaj (1999) suggest that collisional quenching of C(^1D) by water should dominate over radiative decay out to cometocentric distances of ~40,000 km in Hale-Bopp, resulting in little emission from this region. In addition, photoelectrons from H_2O and CO, produced with initial energies in the range of 10–20 eV (Huebner et al. 1992), have a large cross section for collisionally exciting the $\mathrm{C}(^3P) \rightarrow \mathrm{C}(^1D)$ transition (Cosby 1993), although these electrons are rapidly thermalized to much lower energies in the collision zone. The rocket data of McPhate et al. (1999) show evidence of electron impact production of O I] 1356 Å in Hale-Bopp out to distances of 160,000 km, which exceeds the radius of our FOV and implies the presence of electrons with enough energy to produce C(^1D). It follows, therefore, that electron impact excitation can contribute to C(^1D) production throughout the collision sphere to a degree dependent on the variable amount of electron thermalization. Similarly, in the antisunward direction, the role of CO^+ dissociative recombination in C(^1D) production is highly dependent on the properties of the ion tail.

From the above discussion, it is clear that a detailed, self-consistent global model of collisional and photochemical interactions is necessary to fully understand [C I] 9850 Å emission in comet Hale-Bopp. Additional observational studies of C(^1D) from less active comets than Hale-Bopp will also be useful for characterizing the relationship between $Q(H_2O)$ and the role of collisions on the shape of the [C I] 9850 Å coma and the derived Q(CO). As noted above, the Hale-Bopp data set was affected by telescope obscuration, minor etalon misalignment, and high scattered solar continuum from the very dusty coma. Improvements in the FP instrument (Morgenthaler et al. 2002), combined with better sky placement of targets with a more typical gas-to-dust ratio, should result in substantial improvements in sensitivity for less active comets that would be useful to these studies.

We would like to thank F. Roesler for help with configuring the Fabry-Pérot spectrometer, G. Hilton, E. Mierkiewicz, A. Steffl, T. Tillman, and R. C. Woodward for their help observing, and the referee for very helpful comments in preparing this manuscript. This work has been supported under NSF grant AST 96-15625 and NASA grant NAG 5-7952.

REFERENCES

Bhardwaj, A. 1999, J. Geophys. Res., 104, 1929
Biver, N., et al. 1997, Science, 275, 1915
Coakley, M. M., & Roesler, F. L. 1994, Proc. SPIE, 2266, 122
Combi, M. R., Kabin, K., De Zeeuw, D. L., Gombosi, T. I., & Powell, K. G. 1999, Earth Moon Planets, 79, 275
Cosby, P. C. 1993, J. Chem. Phys., 98, 7804
Di Santi, M. A., Mumma, M. J., Dello Russo, N., & Magee-Sauer, K. 2001, Icarus, 153, 361
Feldman, P. D. 1978, A&A, 70, 547
Feldman, P. D., & Brune, W. H. 1976, ApJ, 209, L45
Feldman, P. D., Festou, M. C., Tozzi, G. P., & Weaver, H. A. 1997, ApJ, 475, 829
Festou, M. C. 1984, Adv. Space Res., 4, 165
Fink, U., & Di Santi, M. A. 1990, ApJ, 364, 687
Harris, W. M., Scherb, F., Mierkiewicz, E., Oliversen, R., & Morgenthaler, J. 2002, ApJ, 578, 996
Haser, L. 1957, Bull. Acad. R. Sci. Liège, 43, 740
Hibbert, A., Biemont, E., Godefroid, M., & Vaeck, N. 1993, A&AS, 99, 179
Huebner, W. F., Keady, J. J., & Lyon, S. P. 1992, Ap&SS, 195, 1
McPhate, J. B., Feldman, P. D., McCandliss, S. R., & Burgh, E. B. 1999, ApJ, 521, 920
Morgenthaler, J. P., Harris, W. M., Scherb, F., & Oliversen, R. J. 2002, Earth Moon Planets, in press
Morgenthaler, J. P., et al. 2001, ApJ, 563, 451
Münch, G., & Hippelein, H. 1982, Ann. NY Acad. Sci., 395, 170
Osterbrock, D. E., Fulbright, J. P., & Bida, T. A. 1997, PASP, 109, 614
Roesler, F. L. 1974, in Methods of Experimental Physics, ed. N. P. Carleton (New York: Academic Press), 531
Roesler, F. L., Reynolds, R. J., & Scherb, F. 1995, in IAU Colloq. 149, Tridimensional Optical Spectroscopic Methods in Astrophysics, ed. G. Comte & M. Marcelin (ASP Conf. Ser. 71; San Francisco: ASP), 95
Schultz, D., Li, G. S. H., Scherb, F., & Roesler, F. L. 1992, Icarus, 96, 190
Smyth, W. H., Combi, M. R., Roesler, F. L., & Scherb, F. 1995, ApJ, 440, 349
Swensson, J. W., Benedict, W. S., Delbouille, L., & Roland, G. 1970, The Solar Spectrum from λ 7498 to λ 12016, Vol. 5 (Liège: Soc. R. Sci. Liège)
Tozzi, G. P., Feldman, P. D., & Festou, M. C. 1998, A&A, 330, 753
Weaver, H. A., Feldman, P. D., & McPhate, J. B. 1994, ApJ, 422, 374
Whipple, F. L., & Huebner, W. F. 1976, ARA&A, 14, 143